Journal of Ambient Intelligence and Humanized Computing (2022) 13:2253–2268
https://doi.org/10.1007/s12652-021-02984-6

ORIGINAL RESEARCH

A Markov chain model for IEEE 802.15.4 in time critical wireless sensor networks under periodic traffic with reneging packets

Hossein Hadadian Nejad Yousefi[1] · Yousef Kavian[1] · Alimorad Mahmoudi[1]

Received: 6 October 2020 / Accepted: 27 February 2021 / Published online: 11 March 2021

Abstract

Nowadays, wireless sensor networks (WSNs) and Internet of Things (IoT) employ the IEEE 802.15.4 media access control (MAC) protocol in many applications. In time critical applications with periodic traffic model when the packets have a specified time to live (TTL), if the packet stays in the queue of a sensor node more than time to live, the node should drop that packet, which called reneging packet, to improve the network performance. This paper presents a new analytical Markov model for the IEEE 802.15.4 protocol in non-beacon enabled mode for the periodic traffic considering the reneging packets. The proposed model is applied to the both acknowledged and non-acknowledged modes under heterogeneous traffic for time critical sensor network applications. We obtain the probability distribution function (PDF) of packet delay (PD) and packet delivery ratio (PDR) under periodic and high data rate traffic model. The effects of packet generation period and reneging packets on the performance of sensor network is investigated. The results confirm that dropping an unusable reneging packet increases the network performance, and the non-acknowledged mode can be used for high data rate applications in which the delay is more critical than the packet delivery ratio.

Keywords Markov model · IEEE 802.15.4 · Periodic traffic · Reneging packet · Time critical applications · Performance evaluation · Wireless sensor networks · Internet of Things

1 Introduction

Wireless sensor networks (WSNs) are pervasive technology for distributed computing and measurement. The sensor networks have limited computing capabilities with the intrinsic limitations of wireless communication, consequently low power and low data rate communication protocols are employed for transmitting measured sensor data (Sharif and Kavian 2015).

Recently, wireless sensor networks are employed in multimedia applications with real time and high data rate traffic models (Koyuncu et al. 2019; Yadav et al. 2019). The clustering protocols are promising approaches to improve the performance of sensor networks applications (Zheng et al. 2019). The IEEE 802.15.4 protocol is widely used in WSNs, and recently received much attentions by modern trends Internet of Thing (IoT) and Industry 4.0 applications. Fraile et al. (2020) provided a comparative study of LoRa and IEEE 802.15.4 based IoT inside applications of school buildings. A performance to cost analysis of IEEE 802.15.4 MAC with 802.15.4e MAC modes for IoT applications was presented by Choudhury et al. (2020). Davoli et al. (2018) discussed the challenges and solutions of the integration of IEEE 802.15.4/802.11 and sub-GHz technologies for the IoT applications. Gezer and Okdem (2020) improved the IEEE 802.15.4 channel access performance for IoT and WSN devices.

The IEEE 802.15.4 based wireless sensor technology selection for Industry 4.0. Manufacturing systems was discussed by Badr Mohamed Mahmoud Abdelrehim (2020). The IEEE 802.15.4 as the main part of industrial wireless networks has been considered in the context of Industry 4.0 in (Li et al. 2017). Data management issues and several open research challenges for the IEEE 802.15.4 based networked Industry 4.0 was reviewed in (Raptis et al. 2019). Smart sensors and measurement technology for Industry 4.0 was presented in (Schütze et al. 2018).

The IEEE 802.15.4 protocol supports energy efficient, reliable and timely packet transmissions by tuning the

✉ Yousef Kavian
y.s.kavian@scu.ac.ir

[1] Faculty of Engineering, Shahid Chamran University of Ahvaz, Ahvaz, Iran

parameters of media access control (MAC) layer. According to the characteristics of WSNs and IoT applications, tuning the MAC layer parameters is a difficult task and a statistical model is needed to investigate the impact of the tuning parameters on the network performance (Moulik et al. 2019).

Although many analytical models of the IEEE.802.15.4 protocol has been developed for random traffic models (Misic et al. 2004; Pollin et al. 2006, 2008; Bianchi 2000), the periodic traffic is also common in WSNs applications that should deliver the packets with a specific delay (Farag et al. 2018). For example, industrial wireless sensor networks which designed for real time and time critical applications require timely and deterministic data delivery within stringent deadline bounds. Exceeding delay limits for such applications can lead to system malfunction or ultimately dangerous situations that can threaten human safety (Cao et al. 2015). Hence, according to queuing theory modelling, we define a reneging packet as a packet which leaves the queue before getting service when the waiting time in the queue is more than the deadline. In this case, a reneging packet is a packet whose deadline is over and is an unusable packet that a node should drop that. The number of reneging packets rise in high data rate traffics. When the arrival data rate is greater than the service rate and the queue of node overflows, a node can drop unusable packets to avoid this situation. To the best of our knowledge, there is no prior report about considering the reneging packets in sensor networks modelling. We present an analytical model to evaluate the performance of a sensor cluster based on the IEEE 802.15.4 by considering the effect of reneging packets in high data rate applications. The main contributions of this research work are described as follows:

- Providing a discrete time Markov model for the IEEE.802.15.4 standard in order to obtain the function of sensor nodes as the cluster members.
- Providing an absorbing Markov model for evaluating the effect of parameters on the performance of sensor network.
- Obtaining a cumulative function for packet delay (PD) instead of average which is more important than mean especially for time critical applications.
- Obtaining the probability distribution function (CDF) of packet delay and packet delivery ratio (PDR) with respect to the effect of reneging packets.

The models and simulation results confirm that dropping reneging packets improves the network performance and quality of service requirements. If the deadline of received data is over, the data in not valuable in time critical application and the network should pay more cost for keeping and handling that data. Therefore, by dropping reneging packets, the node can send valuable data to the cluster head.

The rest of paper is organized as follows. Section 2, presents the related works. The system modelling issues and ideas are described in Sect. 3, following that the network performance evaluation are illustrated and discussed in Sect. 4. The analytical and simulation results are presented in Sect. 5. Finally, the paper is concluded in Sect. 6.

2 Related works

In this section, the literature review of related research works is presented. The delay and packet delivery ratio are two important concepts in timely applications of sensor networks. The network calculus studies that estimate certain delay bounds using worst case methods (Burchard et al. 2006; Schmitt et al. 2007) have some limitations in timely application. These bounds are not practical due to the nature of the wireless channel and low power transmission. Furthermore, in timely applications, it is preferred to drop packets with higher delay to service the receiving packets with lower delay (Aoun and Argyriou et al. 2010; Aoun et al. 2011). For these reasons, probabilistic analyses are more suitable than the worst case methods (Wang et al. 2012). In some other research on sensor networks, the simulation models are provided for performance evaluation of IEEE 802.15.4 applications (Rasouli et al. 2014; Ateeq et al. 2019).

Mathematical modeling and probabilistic analysis are indispensable in order to consider the optimum performance of network (Rahimifar et al. 2020). However, queueing systems based on Markov chain model has been used for modeling the wireless sensor networks (Hadadian Nejad Yousefi et al. 2019b), but the first models of the IEEE802.15.4 are especially based on Markov chain models proposed in (Misic et al. 2004; Pollin et al. 2006, 2008) which are in turn based on IEEE802.11 model proposed by Bianchi (2000). In Misic et al. (2004), the authors added transmission and idle states to the Markov chain model recommended by Bianchi (2000), then they evaluated throughput, average delay, energy consumption, average number of backoff stage, and loss packet probability. A modified Markov chain model with limited retransmission for acknowledgment mechanism is proposed in Pollin et al. (2008). The throughput, packet delay, number of backoff, energy consumption and packet delay loss probability are analyzed in Kim et al. (2006) for low rate, non-beacon-enabled and non-saturated traffic. The effect of both uplink and downlink traffic are considered in (Kim et al. 2009; Misic et al. 2006). The performance of IEEE 802.15.4 including the inactive period has been analyzed in (Kim et al. 2016). In Di Marco et al. (2010) and Zhu et al. (2012), the network performance has been investigated under heterogeneous traffic. Some of the works analyzed the star networks, and the rest considered the multi-hop topology for network modelling and performance evaluation. In

Martalò et al. (2009), they have analyzed the star and multi-hop networks using the Markov chain models.

So far, the effect of packet reneging on packet delay and packet delivery ratio in IEEE 802.15.4 has not been modeled and analyzed in wireless sensor networks for time critical applications, such as vehicular safety and industrial networks (Hadadian Nejad Yousefi et al. 2019b; Xu and Guo 2019), which is the main concern and contribution of this research.

3 System model

In this section a general overview of the IEEE 802.15.4 carrier sense multiple access with collision avoidance (CSMA/CA) mechanism and the assumptions which are taken into account in this research work are presented. The IEEE 802.15.4 standard contains the physical (PHY) layer and MAC sublayer specifications for low rate wireless personal area networks (WPANs). This standard uses the binary exponential backoff protocol to reduce collision and two modes to access the channel, i.e. the beacon-enabled (Biswas et al. 2019) and non-beacon-enabled modes (IEEE Standard Association 2015; Biswas et al. 2020).

In this paper, a new analytical model for IEEE802.15.4 CSMA/CA mechanism for the star topologies with heterogeneous and time trigger traffic that has a specific deadline is proposed. The deadline determines the time to live (TTL) of the packet, and when it is over, this packet is valueless even though the node has wasted energy to send that.

3.1 Reneging packets

In recent years, some services need a strict deadline in many applications, such as telecommunication systems with voice and video traffic (Nejad Yousefi et al. 2019a), and real time control systems (Kobayashi 2015). For example, ITU G.114 suggests that end to end delays for interactive voice must be kept below 150 ms. In real time systems, some packets must be sent to the sink in a predefined deadline since delayed data may lead to wrong decisions in the control unit (Tavallaie et al. 2017).

The reneging packets are generated in communication systems that packets must be delivered to the destination before the deadline is over. The sensor node drops the reneging packet and does not need to waste energy to send these packets. The reneging packet dropping will improve the network performance by reducing the consumed energy as well, which has a positive influence on the network lifetime (El-Fouly and Ramadan 2020). Furthermore, the results in Aoun and Argyriou (2010) and Quang and Kim (2012) show that service reneging increases the percentage of packets delivered before the deadline. This is an important performance parameter called deadline delivery success ratio.

3.2 IEEE 802.15.4 non-beacon-enabled CSMA/CA

In the IEEE802.15.4 non-beacon-enabled CSMA/CA mechanism, when a node has data to send, first, as shown in Fig. 1, the MAC sublayer initiates three parameters, namely Number of Backoffs ($NB=0$), Backoff Exponent ($BE=macMinBE$), and Retransmission Times ($RT=0$). Then, the node waits for a random backoff period in the range of [0 2^{BE}-1]. After finishing the backoff period, the node performs a clear channel assessment (CCA). If the channel is idle, the node transmits the packet and wait for acknowledgment (ACK) packet. Then, if the node receives the ACK, the transmission is successful. Otherwise, it resets the value of BE and NB to the initial value and increases the value of RT by one

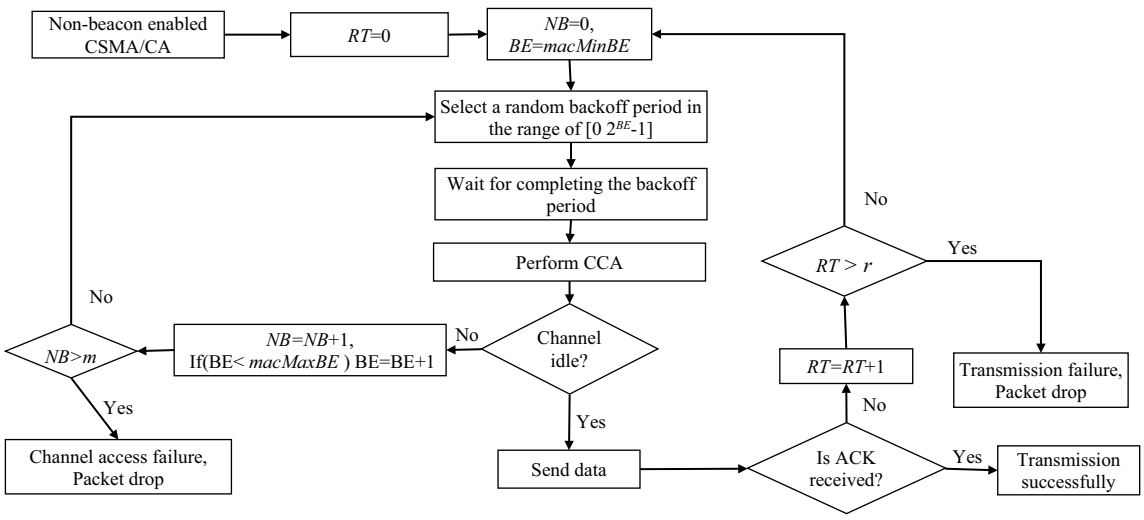

Fig. 1 The mechanism of the IEEE802.15.4 non-beacon-enabled CSMA/CA protocol

unit. Next, the node generates a new random backoff period and repeats the process. If the value of *RT* reaches *macMaxFrameRetries,* the packet is dropped.

When the node performs the CCA, and the channel is not clear, the node increases both values of *NB* and *BE* by one until they reach the maximum values *macMaxCSMABackoffs* and *macMaxBE*, respectively. As the value of *BE* increases, the contention window size is doubled, and consequently, the collision probability decreases. When the value of *NB* reaches *macMaxCSMABackoffs*, the node drapes the packet due to channel access failure. More details are given in (IEEE Standard Association 2015), and a survey of methodology to enhance the performance of the IEEE802.15.4 protocol is provided in Khanafer et al. (2014).

3.3 Markov chain model

In this section, first a Markov chain model is proposed for each transmission attempt in non-beacon-enabled CSMA/CA protocol. The model is extended for finite retransmission and channel assessment for each packet transmission. Then, the model is changed for the non-acknowledged (non-ACK) mode to investigate the impact of ACK on the packet delay and PDR parameters. Finally, the model is extended for some limited tries to get the channel for each packet transmission. For each model, the transmission probability matrix is calculated using the transition probability between the model states.

In order to make an attempt to send a packet, the node selects a random backoff period in the range $[0\ W_{i,j} - 1]$, as shown in Fig. 2., $W_{i,j}$ is the contention window size where i and j are the number of channel access failures and packet retransmissions, respectively. Then, the node executes a CCA and sends a packet if the channel is idle.

The number of the states for each situation is equal to its duration time divided by a specific predefined time interval called backoff slot denoted by $t_{b\text{-}slot}$. Let α be the probability of the channel being busy in CCA and P_c be the probability of collision. Figure 2c represents the whole Markov model depicted in Fig. 2a, and the latter could be replaced by Fig. 2c and called 'building block' henceforth. Likewise, the three blocks Rx/Tx turnaround time, sending and Rx/Tx turnaround time are combined and form 'transmission block' shown in Fig. 2b.

The Markov chain shown in Fig. 3, models the IEEE802.15.4 non-beacon-enabled CSMA/CA protocol with limited retransmission (*RT*) and number backoff (*NB*). This model is constructed by the building blocks, one of them is shown in Fig. 2, and other two situations are the idle state and the states of data transmission from

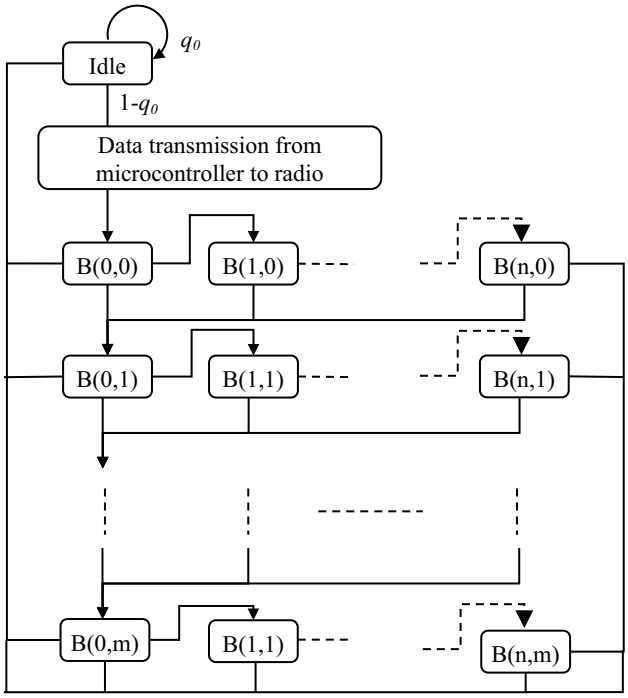

Fig. 3 The Markov chain model for the IEEE802.15.4 non-beacon-enabled CSMA/CA protocol with limited retransmission

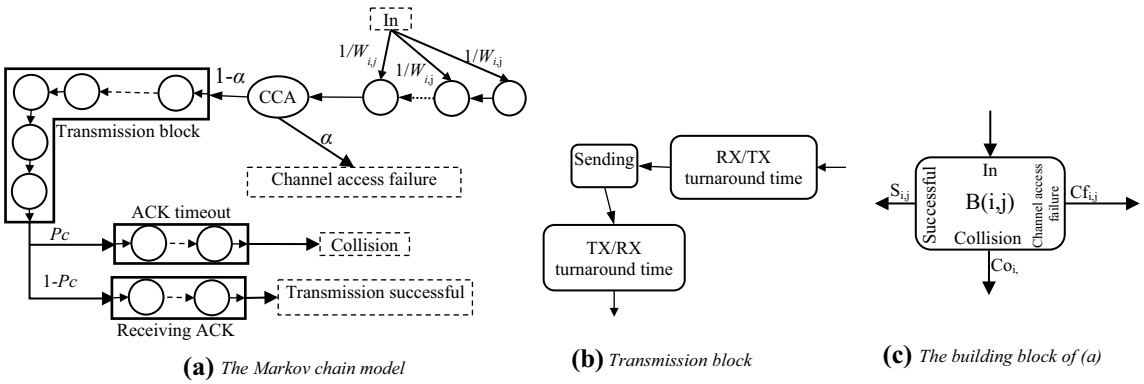

(a) *The Markov chain model* **(b)** *Transmission block* **(c)** *The building block of (a)*

Fig. 2 The Markov chain model for one try to send a packet in the acknowledged mode

a microcontroller to a radio module. According to data transmission protocol between the microcontroller and the radio of wireless node, this situation called 'data shifting situation' in this paper and includes a specified number of states.

All successful outputs of the building blocks connect to the idle state. Some transition lines from successful outputs to the idle state are not drawn in Fig. 3 for better clarity. Let q_0 be the probability of the MAC queue being empty, q_0 is zero in the saturated traffic.

The remaining parts of this section describe how to obtain the transition probability matrix of the final model as shown in Fig. 3. First, the transition probability matrix of the building block denoted by P_{Bi} is obtained from Eq. (1). Then, the transition probability matrix of the final model is acquired from this matrix and the connection between the blocks in the final model.

$$\mathrm{P_{Bi}} = \begin{bmatrix} \mathrm{P_{BA}} & \mathrm{P_{B2C}} & 0 & 0 & 0 \\ 0 & 0 & \mathrm{P_{C2T}} & 0 & 0 \\ 0 & 0 & \mathrm{P_T} & \mathrm{P_{CM}} & \mathrm{P_{SM}} \\ 0 & 0 & 0 & \mathrm{P_{RA}} & 0 \\ 0 & 0 & 0 & 0 & \mathrm{P_{TO}} \end{bmatrix} \tag{1}$$

The following is how to obtain the components of this matrix. $\mathrm{P_{BA}}$ is a $W_{i,j} \times W_{i,j}$ transition probability matrix among the backoff states and is obtained from Eq. (2). $\mathrm{P_{B2C}}$ is a transition probability matrix from the backoff states to the CCA state, and it is a $W_{i,j} \times 1$ column matrix obtained from Eq. (3).

$$\mathrm{P_{BA}} = \begin{bmatrix} 0 & 1 & 0 & \cdots & 0 \\ 0 & 0 & 1 & \cdots & 0 \\ \vdots & \vdots & \vdots & \ddots & \vdots \\ 0 & 0 & 0 & \cdots & 1 \\ 0 & 0 & 0 & \cdots & 0 \end{bmatrix} \tag{2}$$

$$\mathrm{P_{B2C}} = \begin{bmatrix} 0 & \cdots & 0 & 1 \end{bmatrix}' \tag{3}$$

$\mathrm{P_{C2T}}$ is a transition probability vector from the CCA state to the transmission states, and it is a row matrix that obtained from Eq. (4).

$$\mathrm{P_{C2T}} = \begin{bmatrix} 1-\alpha & 0 & \ldots & 0 \end{bmatrix} \tag{4}$$

$\mathrm{P_T}$, $\mathrm{P_{RA}}$, and $\mathrm{P_{TO}}$ are the transition probability matrixes among transmission, receiving ACK, and ACK timeout states, respectively. These matrixes are similar to $\mathrm{P_{BA}}$ with a different size. $\mathrm{P_{CM}}$ and $\mathrm{P_{SM}}$ are transition probability matrixes from transmission states to ACK timeout and receiving ACK states, respectively. Furthermore, $\mathrm{P_{CM}}$ and $\mathrm{P_{SM}}$ are obtained from Eq. (5) and Eq. (6), respectively.

$$\mathrm{P_{CM}} = \begin{bmatrix} 0 & 0 & \cdots & 0 \\ \vdots & \vdots & \ddots & \vdots \\ 0 & 0 & \cdots & 0 \\ P_C & 0 & \cdots & 0 \end{bmatrix} \tag{5}$$

$$\mathrm{P_{SM}} = \begin{bmatrix} 0 & 0 & \cdots & 0 \\ \vdots & \vdots & \ddots & \vdots \\ 0 & 0 & \cdots & 0 \\ 1-P_C & 0 & \cdots & 0 \end{bmatrix} \tag{6}$$

The transition probability matrix of the Markov chain in Fig. 3 is comprised of the transition probability matrix of the building blocks, idle state, data shifting situation, and transitions among them. This matrix is organized by Eq. (7).

$$\mathrm{P_M} = \begin{bmatrix} \mathrm{P_I} & \mathrm{P_{I2D}} & 0 \\ 0 & \mathrm{P_D} & \mathrm{P_{D2B}} \\ \mathrm{P_{B2I}} & 0 & \mathrm{P_B} \end{bmatrix} \tag{7}$$

where $\mathrm{P_{I2D}}$ calculated by Eq. (8), is the transition probability vector from the idle state to the data shifting states and $\mathrm{P_{D2B}}$ obtained from Eq. (9) is the transition probability matrix from the data shifting states to the building block states.

$$\mathrm{P_{I2D}} = \begin{bmatrix} q_0 & 0 & \ldots & 0 \end{bmatrix} \tag{8}$$

$$\mathrm{P_{D2B}} = \begin{bmatrix} 0 & \cdots & 0 & 0 & \cdots & 0 \\ \vdots & \ddots & \vdots & \vdots & \ddots & \vdots \\ 0 & \cdots & 0 & 0 & \cdots & 0 \\ \frac{1}{W_0} & \cdots & \frac{1}{W_0} & 0 & \cdots & 0 \end{bmatrix} \tag{9}$$

$\mathrm{P_{B2I}}$ derived from Eqs. (10–14) is a transition probability matrix from the states of building blocks to the idle state. When a packet is transmitted successfully, the node comes to the idle state from the last state of receiving ACK. Thus, the corresponding element in $\mathrm{P_{B2I}}(i,j)$ is one, as illustrated in Eq. (11). For the building blocks with the last try to get the channel as expressed in Eq. (12), the node also comes to the idle state from the CCA state with the probability α. Equation (13) expresses the node in the last retransmission comes to the idle state from the last state of ACK timeout and receiving ACK. When the node is simultaneously in the last retransmission and the last trying to get the channel, the node comes to the idle state from the end state of receiving ACK, ACK timeout, and CCA with the probability 1, 1, and $1-\alpha$, respectively.

$$\mathrm{P_{B2I}} = \begin{bmatrix} \mathrm{P_{B2I}}(0,0) & \cdots & \mathrm{P_{B2I}}(n,0) & \cdots & \mathrm{P_{B2I}}(0,m) & \cdots & \mathrm{P_{B2I}}(n,m) \end{bmatrix}' \tag{10}$$

$$\mathrm{P_{B2I}}(i,j) = \begin{bmatrix} 0 & \cdots & 0 & 1 & 0 & \cdots & 0 \end{bmatrix}' \; i \neq n, j \neq m \tag{11}$$

$$\mathrm{P_{B2I}}(n,j) = \left[0 \ \cdots \ 0 \ 1 \ 0 \ \cdots \ 0 \ \alpha \ 0 \ \cdots \ 0\right]' \ i = nj \neq m \tag{12}$$

$$\mathrm{P_{B2I}}(i,m) = \left[0 \ \cdots \ 0 \ 1 \ 0 \ \cdots \ 0 \ 1 \ 0 \ \cdots \ 0\right]' \ i \neq nj = m \tag{13}$$

$$\mathrm{P_{B2I}}(n,m) = \left[0 \ \cdots \ 0 \ 1 \ 0 \ \cdots \ 0 \ 1-\alpha \ 0 \ \cdots \ 0 \ 1 \ 0 \ \cdots \ 0\right]' \ i = nj = m \tag{14}$$

$\mathrm{P_D}$ and $\mathrm{P_I}$ obtained from Eq. (15) and (16) are matrixes of transition probability of the data shifting situation and the idle state, respectively. Also, $\mathrm{P_B}$ is a transition probability matrixes among the building blocks, and it is obtained from Eq. (17).

$$\mathrm{P_I} = 1 - q_0 \tag{15}$$

$$\mathrm{P_D} = \begin{bmatrix} 0 & 1 & 0 & \cdots & 0 \\ 0 & 0 & 1 & \cdots & 0 \\ \vdots & \vdots & \vdots & \ddots & \vdots \\ 0 & 0 & 0 & \cdots & 1 \\ 0 & 0 & 0 & \cdots & 0 \end{bmatrix} \tag{16}$$

$$\mathrm{P_B} = \begin{array}{c} \\ \mathrm{B}(0,0) \\ \vdots \\ \mathrm{B}(n,0) \\ \vdots \\ \mathrm{B}(0,m) \\ \vdots \\ \mathrm{B}(n,m) \end{array} \begin{bmatrix} \mathrm{P_{B}}_i & \mathrm{P_{B}}_{i+1} & \cdots & 0 & \mathrm{P_{B}}_{j+1} & \cdots & 0 & 0 & \cdots & 0 \\ \vdots & \vdots & \ddots & \vdots & \vdots & \cdots & \vdots & \vdots & \ddots & \vdots \\ 0 & 0 & \cdots & \mathrm{P_{B}}_i & \mathrm{P_{B}}_{j+1} & \cdots & 0 & 0 & \cdots & 0 \\ \vdots & \vdots & \ddots & \vdots & \vdots & \ddots & \vdots & \vdots & \ddots & \vdots \\ 0 & 0 & \cdots & 0 & 0 & \cdots & \mathrm{P_{B}}_i & \mathrm{P_{Bi+1}} & \cdots & 0 \\ \vdots & \vdots & \ddots & \vdots & \vdots & \vdots & \vdots & \vdots & \ddots & \vdots \\ 0 & 0 & \cdots & 0 & 0 & \cdots & 0 & 0 & \cdots & \mathrm{P_{B}}_i \end{bmatrix} \tag{17}$$

where $\mathrm{P_{B}}_{i+1}$ and $\mathrm{P_{B}}_{j+1}$ are transition probability matrixes from a building block to next building block when the channel is busy and retransmission number reaches the maximum, respectively. All elements of $\mathrm{P_{B}}_{i+1}$ are zero except the elements corresponding with transition from CCA to each backoff states. These probabilities are equal to $\alpha/W_{i,j}$. $\mathrm{P_{B}}_{j+1}$ is similar to $\mathrm{P_{B}}_{i+1}$ with the exception that the non-zero elements are the probabilities of transition from the last state of ACK timeout states to each backoff states and these are equal to $1/W_{i,j.}$

The transition probability matrix of the Markov chain model is obtained by replacing Eqs. (8–17) in Eq. (7). The matrix depends on the two parameters P_C and α. The former is the collision probability, and the latter is the probability of the channel being busy in CCA.

With the main assumption that the probability of a node decides to transmit a packet is independent of other nodes (Pollin et al. 2006, 2008; Park et al. 2013), the channel is busy in a CCA when at least one node is sending a packet into the channel or the base station is sending ACK packet. In the other words, the channel is clear when no node is sending a packet into the channel. The probability that the channel is busy is obtained from Eq. (18).

$$1 - \alpha = \prod_{i=1}^{n-1}(1 - (\tau_i(1-\alpha_i)(L_{pcki} + L_{acki}(1 - P_{ci})) \tag{18}$$

where n is the number of nodes in the star network and τ_i is the summation of the steady state probabilities that node i is in the CCA states. L_{pcki} and L_{acki} are the number state of the transmission and receiving ACK block for node i, respectively. In other words as in Eq. (19), the collision probability is equal to the probability of other nodes have no decision to send a packet (Kim et al. 2009).

$$P_C = (1 - \prod_{i=1}^{n-1}(1 - \tau_i)) \tag{19}$$

The values of P_C and α also depend on τ_i. As a result, α, $\tau_{i,}$ and P_C cannot be determined without knowing about each other. Therefore, an iterative procedure is conducted to determine these parameters.

First, α and P_C of each node are set to initial values. After that, the Markov chain is constructed by using the initial value of α and P_C. Then, τ_i is calculated based on the steady-state probability of the model. Next, the values of α and P_C are updated with the new value of τ_i. Afterward, τ_i is calculated with updated α and P_C. This procedure is performed iteratively until the difference between the two successive iterations for all parameters is negligible. As a result, the transition probability matrix of the general Markov chain model $\mathrm{P_M}$ is obtained.

3.4 Non-acknowledged model

In the non-acknowledged mode, when a data packet is sent, the node is not waiting to receive the ACK packet. The proposed Markov chain model for one try to send data in the non-ACK mode of the IEEE802.15.4 is depicted in Fig. 4.

The transition probability matrix of the non-ACK mode is the modified $\mathrm{P_{Bi}}$ and is obtained from Eq. (20).

$$\mathrm{P}_{B'i} = \begin{bmatrix} \mathrm{P_{BA}} & amp;\mathrm{P_{B2C}} & amp;0 \\ 0 & amp;0 & amp;\mathrm{P_{C2T}} \\ 0 & amp;0 & amp;\mathrm{P_T} \end{bmatrix} \tag{20}$$

The Markov chain model for a limited number of channel access failure is depicted in Fig. 5. The transition probability matrix of this Markov chain model is derived from Eq. (21).

$$P_{M'} = \begin{bmatrix} P_I & P_{I2D} & 0 \\ 0 & P_D & P_{D2B'} \\ P_{B'2I} & 0 & P_{B'} \end{bmatrix} \tag{21}$$

where $\mathrm{P_{B'}}$, $\mathrm{P_{D2B'}}$ and $\mathrm{P_{B'2I}}$ are defined similarly to the previous section, but they have slight differences in size and some elements. They are obtained as follows:

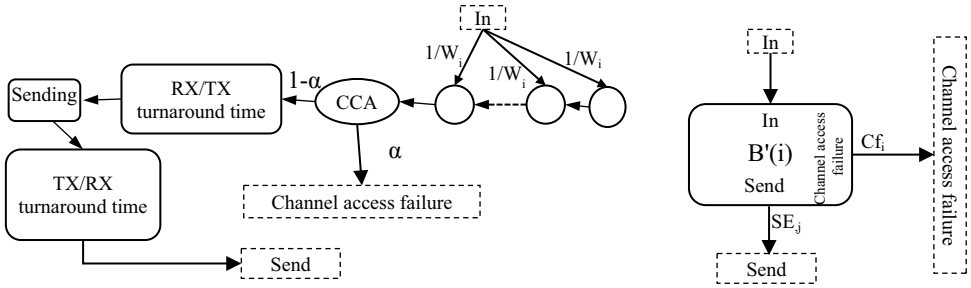

(a) The Markov chain model **(b)** The block of (a)

Fig. 4 The Markov chain model for the IEEE802.15.4 non-beacon-enabled and non-ACK CSMA/CA protocol for one try

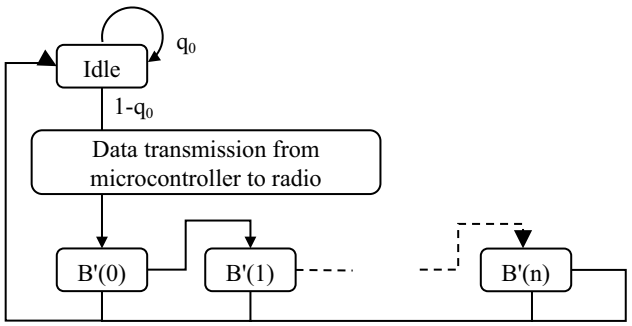

Fig. 5 The Markov chain model for the IEEE802.15.4 non-beacon-enabled non-ACK CSMA/CA protocol with limited channel assessment

$$P_{B2I} = \left[P_{B'2I}(0) \ \cdots \ P_{B'2I}(n)\right]' \tag{22}$$

$$P_{B'2I} = \left[\ 0 \cdots 0 \ \ 1 \ 0 \ \cdots \ 0\right]' \quad i \neq n \tag{23}$$

$$P_{B'2I}(n) = \left[\ 0 \cdots 0 \ \ 1 \ 0 \ \cdots 0 \quad \alpha' \quad 0 \quad \cdots \quad 0\right]' \tag{24}$$

$$P_{B'} = \begin{matrix} B'(0) \\ \vdots \\ B'(n) \end{matrix} \begin{bmatrix} P_{B'i} & P_{B'i+1} & \cdots & 0 \\ \vdots & \vdots & \ddots & \vdots \\ 0 & 0 & \cdots & P_{B'i} \end{bmatrix} \tag{25}$$

where $P_{B'i+1}$ is a transition probability matrix from one building block to the next building block due to the channel access failure.

The transition probability matrix of the non-ACK mode is characterized by one probability value α' from Eq. (26). In this case, the channel is busy when at least one node is sending a data packet to the channel.

$$1 - \alpha' = \prod_{i=1}^{n-1} \left(1 - (\tau_i'(1 - \alpha_i')L_{pcki}\right) \tag{26}$$

The transition probability matrix for the Markov chain model depends on the value of α'. Also, the value of α' depends on the value of τ'_i. Similar to the abovementioned procedure, the value of α' and τ'_i can be determined using the iterative procedure.

4 Performance evaluation

In the previous sections, two generalized Markov chain models were proposed for the CSMA/CA mechanism in two modes: acknowledged mode and non-acknowledged mode. Then, the transition probability matrix, α, and P_C are calculated for both modes.

In this section, the delay of successful delivered packets and PDR are obtained using the properties of absorbing Markov chain models. An absorbing Markov chain is a Markov chain in which every state can reach an absorbing state. An absorbing state is a state with at least one entered and no exit. The absorbing Markov chains are used to generate the probability generating function (PGF) of packet delay.

After obtaining the transmission matrix of Markov chains presented in the previous section, the transition probability matrixes of the absorbing models are achieved for the acknowledged and non-acknowledged mode by Eq. (27) and (28), respectively. As shown in Fig. 6 for acknowledged mode, there are three absorbing states: successful transmission, transmission failure due to channel busy, and maximum retransmission, whereas in the non-acknowledged mode shown in Fig. 7, there are two absorbing states: successful sending and transmission failure due to channel busy.

One of the characteristics of the proposed absorbing models is that they may obtain the probability of reaching any of the absorbing states with the assumption of starting from the idle state. It is also possible to obtain the probability of entrance to the absorbing states after each transition.

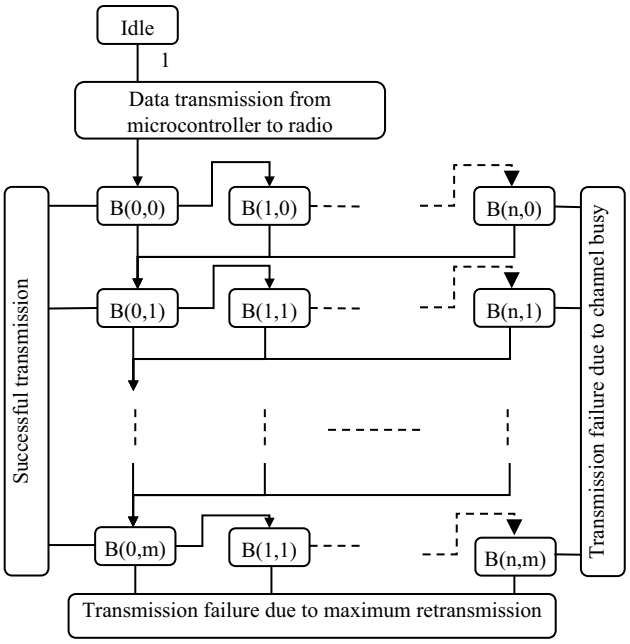

Fig. 6 The absorbing Markov chain model for the IEEE802.15.4 non-beacon-enabled CSMA/CA protocol with limited retransmission

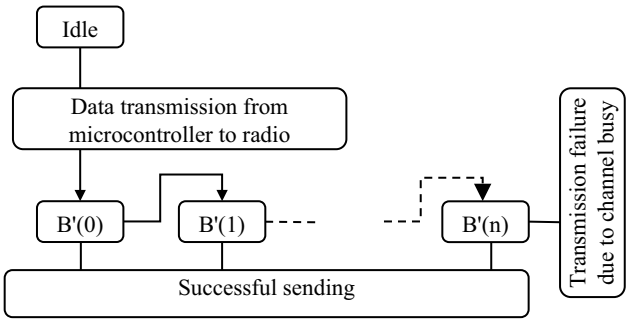

Fig. 7 The absorbing Markov chain model for the IEEE802.15.4 non-beacon-enabled non-ACK CSMA/CA protocol with limited channel assessment

The properties are used to obtain the parameters of delay and PDR in continuation. In this models, q_0 is zero as these parameters are measured when the node generates the packet and transitions from the idle state to the next state.

$$P_{AM} = \begin{bmatrix} P_I & P_{I2D} & 0 & 0 & 0 & 0 \\ 0 & P_D & P_{D2B} & 0 & 0 & 0 \\ 0 & 0 & P_B & P_{B2S} & P_{B2C} & P_{B2A} \\ 0 & 0 & 0 & 1 & 0 & 0 \\ 0 & 0 & 0 & 0 & 1 & 0 \\ 0 & 0 & 0 & 0 & 0 & 1 \end{bmatrix} \quad (27)$$

where P_{B2S}, P_{B2C}, and P_{B2A} are the probability matrixes of transition from the building blocks to the absorbing states which respectively named successful transmission, transmission failure due to channel busy, and transmission failure due to maximum retransmission.

$$P_{AM'} = \begin{bmatrix} P_I & P_{I2D} & 0 & 0 & 0 \\ 0 & P_D & P_{D2B'} & 0 & 0 \\ 0 & 0 & P_{B'} & P_{B'2S} & P_{B'2A} \\ 0 & 0 & 0 & 1 & 0 \\ 0 & 0 & 0 & 0 & 1 \end{bmatrix} \quad (28)$$

where $P_{B'2S}$ and $P_{B'2A}$ are the probability matrixes of transition from the building blocks to the two absorbing states respectively named successful sending and transmission failure due to channel busy.

4.1 Packet delay model

The packet delay model is obtained from the absorbing models, and it is defined as the interval that the process starts in the idle state until reaching the successful transmission. Let i be the number of steps that the absorbing Markov chain model starts in the idle state and moves successively to other states. The probability that the absorbing Markov chain is in each state after i steps is calculated with the assumption of starting in the idle state with respect to the property of absorbing Markov chain models. For example, when the probability of the successful state is 0.1 after 5 steps, it means the probability that the chain is in the successful transition state is 0.1 in the interval [0, 5 × step time]. The step time $t_{b\text{-}slot}$ is defined to construct the Markov chain in Sect. 3. Thus the probability of each absorbing state after i steps can be obtained from Eqs. (29)-(32).

$$U_{int} = \begin{bmatrix} 1 & 0 & \cdots & 0 \end{bmatrix} \quad (29)$$

$$U_1 = U_{int} \times P_{AM} \quad (30)$$

$$U_i = U_{i-1} \times P_{AM} \quad (31)$$

where U_{int} is the initial probability vector which specifies the idle state as the starting state, U_1 is a vector to present the probability of each state after one step with the assumption of starting in the idle state, also U_i is a vector that shows the probability that the Markov chain, starting in the idle state, is in each state after i steps. The final probability of the absorbing states is obtained from U_i after a finite number of steps. The final value of the U_i is denoted by U_{im} whose elements are zero except the elements corresponding with the absorbing states.

The probability generating function of delay is used to obtain the cumulative distribution function of delay. The PGF of delay is obtained from the proposed absorbing Markov chain models illustrated in Figs. 6, 7 for

acknowledged and non-acknowledged modes, respectively. The PGF of packet service time, denoted by $G_T(z)$, is obtained from Eq. (32) and (33) regardless of whether or not the packet is sent successfully.

$$G_T(z) = \sum_{i=0}^{M_0} g_{Ti} \times z^i \tag{32}$$

$$g_{Ti} = U_i(\mathrm{Tr}) - U_{i-1}(\mathrm{Tr}) \tag{33}$$

where $U_i(\mathrm{Tr})$ is the sum of elements corressponding to the all absorbing states in U_i matrix. Thus, g_{ti} is the probability of entrance to all absorbing states in ith step. The PGF of packet service time can express the probability density function for the delivered packet delay when the node has only one packet to send. Let $F_s(z)$ be the PGF of packet delay obtained from Eq. (34–36) when the queue is empty.

$$F_s(z) = \sum_{i=0}^{M_0} f_{si} \times z^i \tag{34}$$

$$ps_i = U_i(\text{succesful transmission}) - U_{i-1}(\text{succesful transmisson}) \tag{35}$$

$$f_{si} = \frac{ps_i}{U_{im}(\text{successful transmission})} \tag{36}$$

where f_{si} is the probability of the successful transmission in the ith step under the condition that the packet is successfully sent, and M_0 is a step number after that the f_{si} is equal to zero. U_i (successful transmission) is the probability of entrance to the successful transmission state from the idle state after i steps, and ps_i is the probability of entrance to the successful transmission state in the ith step. Equation (34) is used to normalize the PGF of packet delay.

The PGF of delay for the nth generated packet is proportional to the period of packet generation denoted by T_S. That is calculated from recursive Eqs. (37–41) and is denoted by F_{s_n}. The subscript n corresponds to the nth generated packet.

$$G_{s\_n}(z) = \sum_{i=0}^{M_n} g_{si\_n} \times z^i \tag{37}$$

$$h_{s0\_n} = \sum_{i=0}^{T_S} g_{si\_n-1} \tag{38}$$

$$H_{s\_n} = h_{s0\_n} + \sum_{i=0}^{M_{n-1}-T_S} g_{s(i+T_P)\_n-1} \times z^{i+1} \tag{39}$$

$$G_{s\_n+1}(z) = G_s(z) \times H_{s\_n} \tag{40}$$

$$F_{s\_n+1}(z) = F_s(z) \times H_{s\_n} \tag{41}$$

where M_n is the number of the elements of G_{s_n}, and h_{s0_n} is the probability that the previous packet is sent before the nth packet is generated. In other words, h_{s0_n} in Eqs. (38–39) represents the probability that the queue is empty exactly when the next packet arrives. Let H_{s_n} be the PGF that the queue of a node becomes empty when the node generates the nth packet. The second term in Eq. (39) is the PGF that the queue is empty, and it is obtained from the PGF of service time of the previous packet which is shifted as much as T_S. Equations (40) and (41) are based on this principle that the probability of servicing to the next packet is equal to the probability of servicing to a packet when the queue is empty multiply by the probability that the queue is empty. In Eq. (40), the service is defined regardless of whether or not the packet is sent successfully, but in Eq. (41) it is defined as the packet is successfully sent.

If the limit of F_{s_n} is finite when n approaches infinity, the average of queue length is also finite; otherwise, it is infinite.

For data having a deadline for delivering to the destination, when the deadline is over, it is worthless. Consequently, the node consumes an amount of energy to send worthless packets and this decreases the network performance. If the node drops worthless packets, it can send usable packet instead of unusable packet (Aoun and Argyriou et al. 2010; Aoun et al. 2011).

The PGF of packet delay with reneging packet is calculated from recursive equations Eqs. (42–47) and it is denoted by $FR_{s\_n}(z)$.

$$G_{T\_n} = \sum_{i=0}^{M_n} g_{Ti\_n} \times z^i \tag{42}$$

$$k_{T0\_n} = \sum_{j=0}^{T} g_{Tj\_n-1} \tag{43}$$

$$k_{Tm\_n} = \sum_{i=M_{k+1}}^{M_n} g_{Ti\_n} \tag{44}$$

$$K_{T\_n}(z) = k_{s0\_n} + k_{Tm\_n} + \sum_{i=1}^{M_k} g_{T(i+T_P)\_n-1} \times z^i \tag{45}$$

$$G_{T\_n}(z) = G_T(z) \times K_{T\_n}(z) \tag{46}$$

$$FR_{s\_n}(z) = \frac{F_s(z) \times K_{T\_n}(z)}{U_{im}(\text{successful transmission})} \tag{47}$$

In these recursive equations, Eq. (43) expresses the probability that the previous packet serviced before T_S is defined by k_{0_n}. From the view of a new packet, k_{0_n} is appeared in the probability that the queue will be empty exactly when it arrives. Furthermore, the probability that the previous packet serviced after the deadline as expressed by k_{Tm_n} in Eq. (44) is appeared in Eq. (45) to show the probability that the queue will be empty exactly when the next packet arrives. The third term in Eq. (45) expresses that the PGF of the empty queue is obtained from the sending PGF of the previous packet which is shifted as much as T_S. Equations (46) and (47) are obtained similar to Eq. (39). The denominator in Eq. (47) is for normalization.

It should be noted that the maximum size of K_{T_n}, denoted by M_k, is proportional to the packet deadline and time unit in the Markov chain analysis. If the packet deadline and time unit are T_d and T_u, respectively, the maximum size of K_T is equal to T_d divided by T_u.

In this case, for every period of packet generation, the node is stable because the node drops the packet, if its waiting time in the queue is larger than the deadline. The average of delay is calculated from Eq. (48) by the property of the PGFs.

$$D_{avg} = F'_{s\_n}(1) \times \text{Time\_slot} \tag{48}$$

Using Little's Law, the length of queue is obtained from Eq. (49).

$$L_{avg} = \frac{D_{avg}}{T_S} \tag{49}$$

4.2 Packet delivery ratio

In this paper, the packet delivery ratio (PDR) is defined as the ratio of the number of valuable packet transmission to the total number of packet transmission. A valuable packet is a delivered packet before its deadline is over. First, the ratio of packet loss is obtained from the absorbing Markov chain. Then, PDR is obtained from the final probability of the absorbing states. The final probability of successful transmission state is used to obtain the PDR for acknowledged mode where expressed in Eq. (50).

$$\text{PDR} = P_{im}(successfultransmission) \tag{50}$$

For non-acknowledged mode, the PDR′ is attained from Eq. (51).

$$\text{PDR}' = P'_{im}(successfultransmission) \times P'_C \tag{51}$$

The PDR for data with a deadline can be obtained from Eq. (52) by using $G_{T\_n}(z)$ that shows the PGF of the packet service time for the nth generated packet.

$$\text{PDR} = P_{im}(successfultransmission) \times \lim_{n\to\infty} \sum_{j=0}^{M_K} g_{Tj\_n} \tag{52}$$

where the second term is the probability that a packet is serviced before the deadline.

5 Model validation and performance analysis

For model validation, the star network is simulated by OMNET + + simulator. Then, the simulation results are compared with the analytical results. Also, the network is composed of 10 sensor nodes in two classes including 7 nodes for class-one and 3 nodes for class-two. The class-one sensor nodes generate packets with low rate traffic $q_0 = 0.9$, and it is assumed that the class-two sensor nodes always have packets to send.

First, the parameters α, P_C and matrix P_M of the proposed Markov chain model are calculated. Then the absorbing Markov chain is constructed and the delay for successful delivered packet and PDR are calculated. The key parameters of the evaluation are listed in Table 1. The effects of data packet generation period on the packet delay and PDR are investigated in the acknowledged mode and non- acknowledged mode.

The CDF of packet delay is obtained for different rates of packet generation for class-two sensor nodes. When the packet generation rate is higher than a threshold rate, the node cannot timely serve the packets, and the queue length approaches infinity. The low rate and high rate are defined as the rate lower and higher than the threshold rate, respectively. When the packet generation rate is low, the node can send a packet with a slight delay. For high rate packet generation, the delay significantly increases because the packet arrives shortly and there is an increase in its waiting time in the queue. Figure 8 illustrates the CDF of the *nth* generated

Table 1 The key parameters of model

Parameter	Value	Parameter	Value	Parameter	Value	Parameter	Value
Radio ra/l//knge	15 m	Bitrate	250 kbps	*macMaxCS-MABackoffs*	5	*macMaxBE*	5
Carrier Frequency	2.412e + 9 Hz	DATA	120 bytes	*macMaxF-rmeRetries*	3	*macMinBE*	3

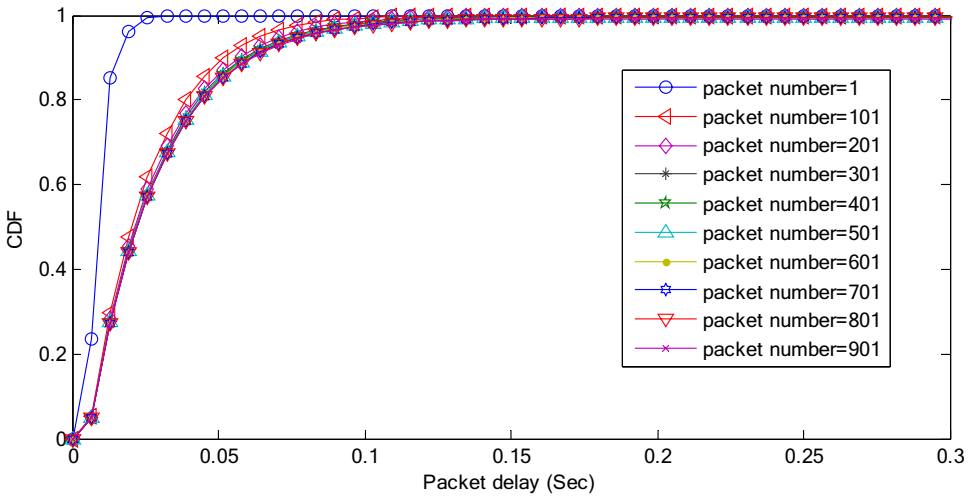

Fig. 8 The CDF of packet delay for the *nth* packet generation for T = 0.02 s

packet when the period of the packet generation is equal to 0.02 s. In this case, the CDFs of packet delays converge very quickly, and the PDR and the average of queue length are equal to 0.91 and 1.85, respectively.

Figure 9 shows the CDF of packet delay when the period of packet generation is equal to 0.018 s. As shown in Fig. 9, the CDFs of packet delays converge more slowly when the period of packet generation is decreased. The PDR and the average of queue length are equal to 0.9 and 6.65, respectively.

Figure 10 shows the CDF of packet delay for two packet generation periods. When the period is decreased, the delay increases. The simulation and analytical results for low data rate are listed in Table. 2. The analytical results are very close to the simulation results.

When the period of packet generation is smaller than a threshold value, the queue length is considered unstable because the arrival packet rate will be larger than the average service time. Figure 11 shows the CDF of packet delay when the period of packet generation is equal to 0.015 s.

The simulation results in Fig. 12 show the packet delay versus the simulation time. In this case, the packet delays increase when the packet generation period decreases and the service time is increased. Thus, the queue length has increased while the packet deadline is over, so the packet is unusable. If this packet is dropped, usable packets can be sent instant of those. As a result, network performance is improved.

According to Figs. 8, 9, 10, 11, 12, when the packet generation period decreases, the channel becomes busier, and as a result, the service time increases. Increasing service time and reducing the packet generation period will increase the probability of entering the packet before the departure of the previous packets. The increasing of the probability, initially causes the CDF of packet delay converges slowly and, with further increases, causes that does not converge.

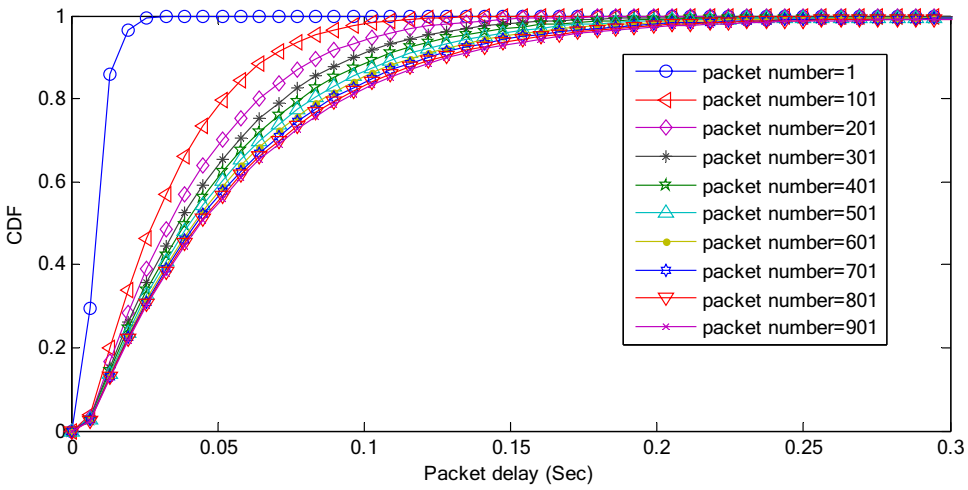

Fig. 9 The CDF of delay for the nth packet generation for T = 0.018 s

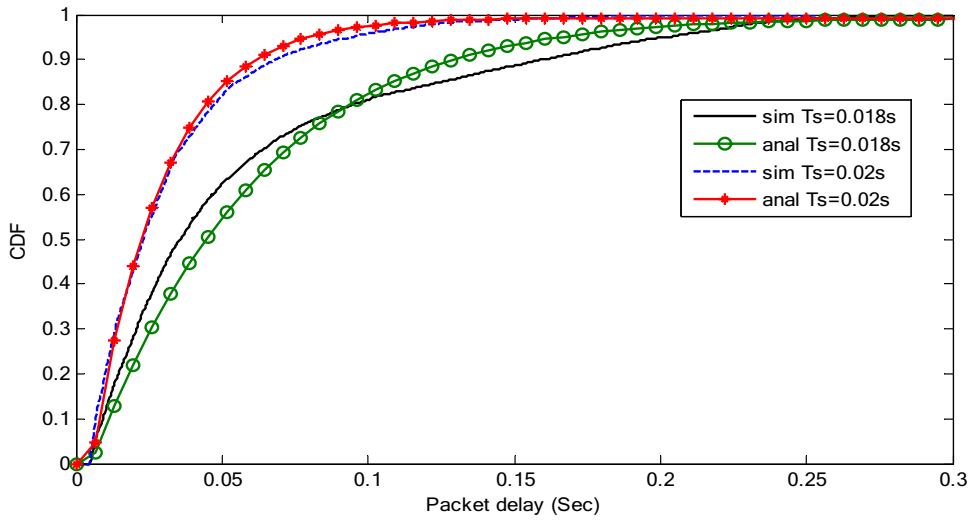

Fig. 10 The CDF of packet delay for low date rate

Table 2 PDR and delay for low date rate

Parameters	Analysis $T_S = 0.018$ s	Simulation $T_S = 0.018$ s	Analysis $T_S = 0.02$ s	Simulation $T_S = 0.02$ s
PDR	0.90%	0.87%	0.91%	0.91%
D_{avg}	0.059 s	0.059 s	0.018 s	0.019 s

Also, this process can be described by Eq. (39). When the packet generation period decreases, the upper limit of summation is increased, so the maximum power of z is increased. Therefore, the maximum power of z is also increased in $F_{s\_n}(z)$ expressed by Eq. (41). Increasing this power decreases the convergence of $F_{s\_n}(z)$ and finally causes the divergence of $F_{s\_n}(z)$.

In high data-rate, when the arrival packet rate is bigger than the average service time, the queue length is unstable. The real time data has a deadline within which they have to be delivered to the destination. When the node drops the unusable packet, the analysis result shows the queue length will be stable. As shown in Fig. 13, the CDFs of packet delay converge, and their average delay is smaller than the deadline. The simulation and analytical result for high data rate with reneging packets are shown in Fig. 14, and their PDR and delay parameters are compared in Table. 3. The deadline is selected to 0.15 s. In this case, the upper limit of summation in Eq. (45) is constant, unlike in Eq. (39). Thus, $FR_{s\_n}(z)$ converges for each packet generation period.

When the non-ACK mode is used to send packets, the PDR decreases while the delay of packet delivery decreases. The simulation results for non-ACK mode show that the average delay decreases while there is a decrease in the PDR. The non-ACK mode can be used for real time data whose delay is more critical than their PDR. Figure 15 depicts the verification of the analysis results in non-ACK mode by simulation. The PDR and average delay parameters are inserted in Table. 4, and the results express the accurate of the proposed analysis method.

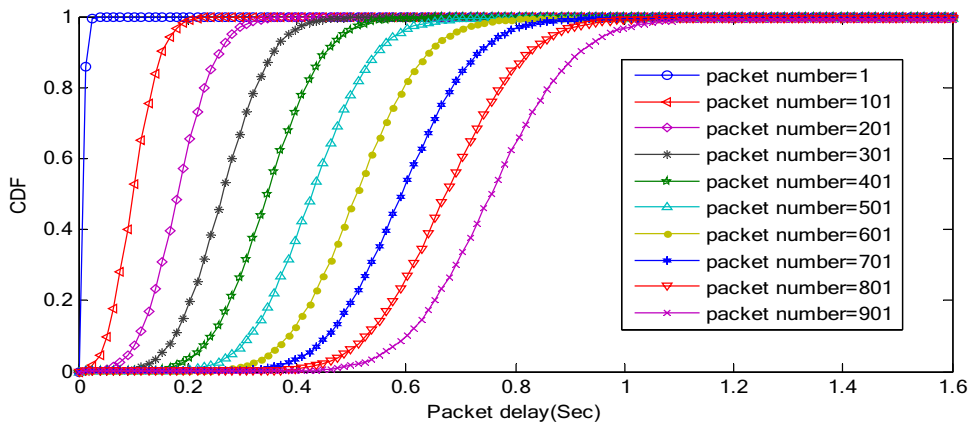

Fig. 11 The CDF of delay for the nth packet generation for $T = 0.013$ s

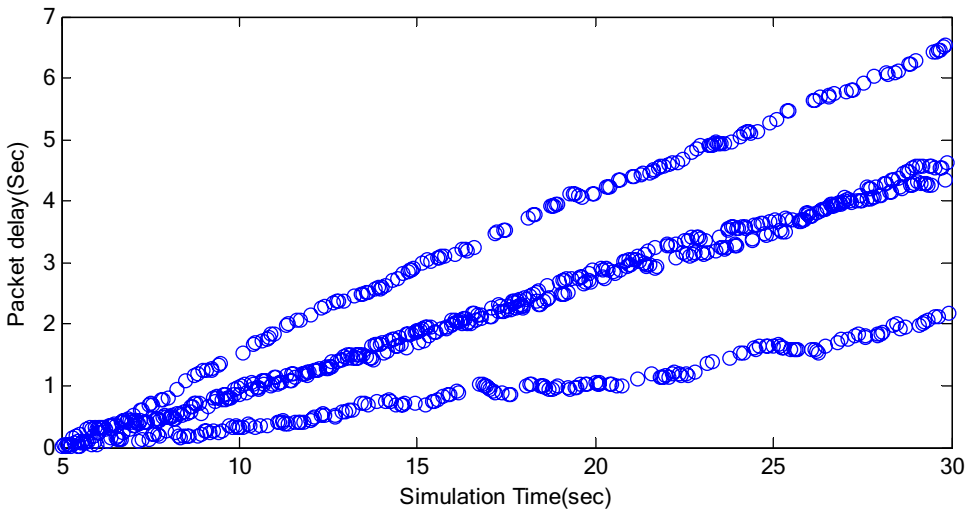

Fig. 12 The delay of packet versus the simulation time for $T = 0.013$ s

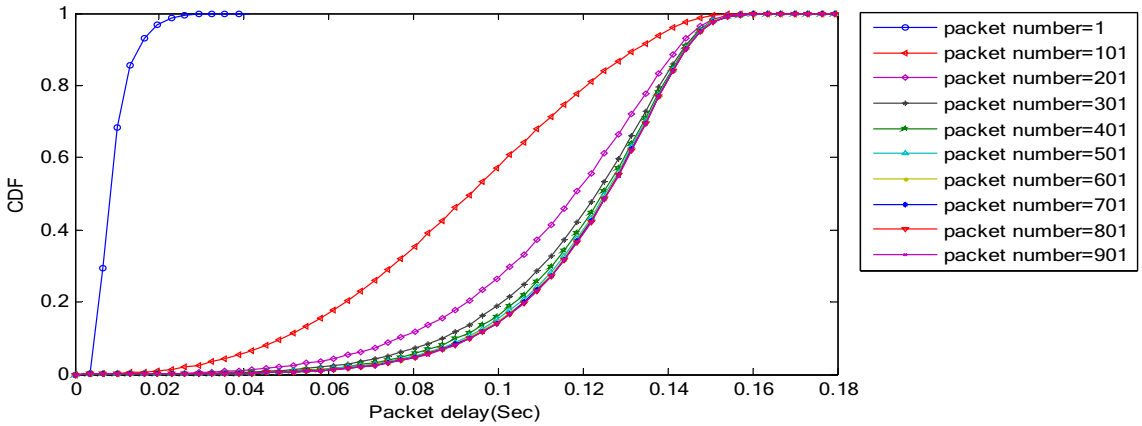

Fig. 13 The CDF of delay for the nth packet generation for T = 0.013 s and deadline = 0.15 s

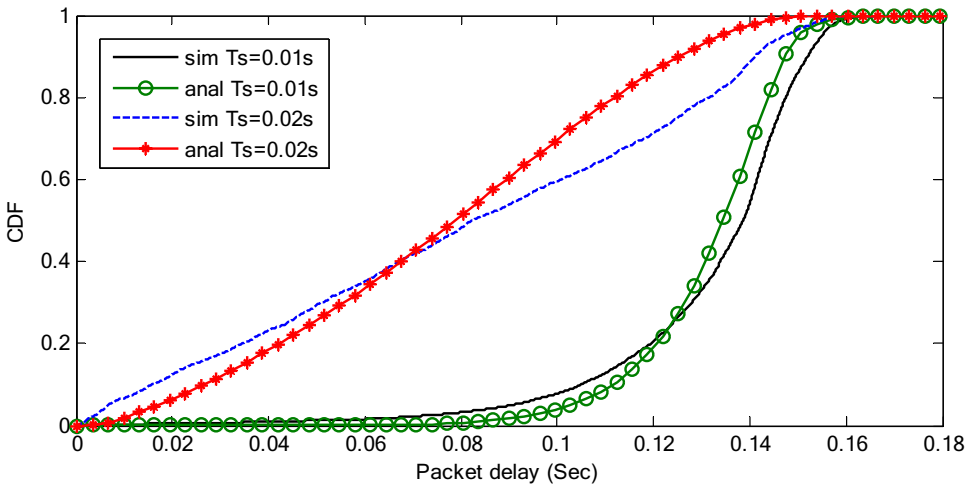

Fig. 14 The CDF of delay for high rate data generation for Ts = 0.015 s and Ts = 0.01 s with deadline = 0.15 s

Table 3 PDR and delay for high date rate

Parameters	Analysis $T_S = 0.01$ s	Simulation $T_S = 0.01$ s	Analysis $T_S = 0.015$ s	Simulation $T_S = 0.015$ s
PDR	0.56%	0.55%	0.78%	0.74%
D_{avg}	0.14 s	0.144 s	0.083 s	8.9 ms

Table 4 PDR and delay for high date rate in non-ACK mode

Parameters	Analysis $T_S = 0.01$ s	Simulation $T_S = 0.01$ s	Analysis $T_S = 0.015$ s	Simulation $T_S = 0.015$ s
PDR	0.70%	67%	0.748%	0. 765%
D_{avg}	11.8 ms	12.2 ms	8.7 ms	8.74 ms

6 Conclusion

In this paper, an analytical Markov model was proposed for IEEE802.15.4 MAC protocol for time critical sensor networks under periodic traffic with reneging packets. The probability distribution function of packet delay and packet delivery ratio were provided when packets have a specified time to live. The analytical model and OMNET + + simulation results confirm that for real time traffic, the average queue length approaches infinity when the packet generating rate is higher than a threshold value. When a node drops unusable reneging packets, the average queue length tends to finite. The non-acknowledged mode is appropriate for real time traffic applications that needs a specific time to be delivered to the destination and in which the delay is more critical than the packet delivery ratio. For future works, the proposed model could be extended to provide other network parameters such as energy consumption, throughput, and reliability. Furthermore, other standard MAC protocols and cluster tree network topology could be considered to extend the model.

Acknowledgements This work was supported by Shahid Chamran University of Ahvaz under Grant Number 98/3/05/14909.

References

Abdelrehim BMM (2020) Wireless sensor technology selection for I4.0 manufacturing systems. Msc Thesis, University of Windsor, CA

Aoun M, Argyriou A (2010) Network coding and service reneging for real-time communication in sensor networks. In: 2010 IEEE Glob Telecommun Conf GLOBECOM 2010, IEEE, 2010: pp. 1–6. doi:https://doi.org/10.1109/GLOCOM.2010.5683091.

Aoun M, Argyriou A, van der Stok P (2011) Performance evaluation of network coding and packet skipping in IEEE 802.15.4-based real-time wireless sensor networks. Wirel Sens Netw. https://doi.org/10.1007/978-3-642-19186-2_7

Ateeq M, Ishmanov F, Afzal MK, Naeem M (2019) Predicting delay in IoT using deep learning: a multiparametric approach. IEEE Access 7:62022–62031. https://doi.org/10.1109/ACCESS.2019.2915958

Bianchi G (2000) Performance analysis of the IEEE 802.11 distributed coordination function. IEEE J Sel Areas Commun 18:535–547. https://doi.org/10.1109/49.840210

Biswas S, Roy SD, Chandra A (2019) Cross-layer energy model for beacon-enabled 802.15.4 networks. J Ambient Intell Hum Comput 10:4209–4224. https://doi.org/10.1007/s12652-018-0923-z

Biswas S, Roy SD, Chandra A (2020) Cross-layer energy model for non-beacon-enabled IEEE 802.15.4 networks. IEEE Wirel Commun Lett 9(7):1084–1088. https://doi.org/10.1109/LWC.2020.2981308

Burchard A, Liebeherr J, Patek SD (2006) A min-plus calculus for end-to-end statistical service guarantees, IEEE Trans. Inf Theory 52:4105–4114. https://doi.org/10.1109/TIT.2006.880019

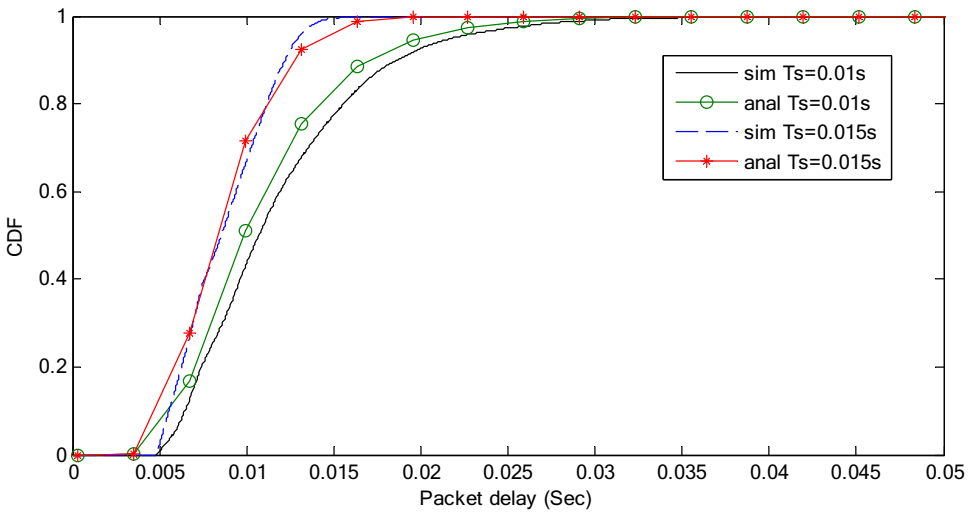

Fig. 15 The CDF of packet delay for non-ACK mode

Cao X, Chen J, Cheng Y, Shen X, Sun Y (2015) An analytical MAC model for IEEE 802.15.4 enabled wireless networks with periodic traffic. IEEE Trans Wirel Commun 14:5261–5273. https://doi.org/10.1109/TWC.2015.2435006

Choudhury N, Matam R, Mukherjee M, Lloret J (2020) A performance-to-cost analysis of IEEE 802.15.4 MAC with 802.15.4e MAC modes. IEEE Access 8:41936–41950. https://doi.org/10.1109/ACCESS.2020.2976654

Davoli L, Belli L, Cilfone A, Ferrari G (2018) From micro to macro IoT: challenges and solutions in the integration of IEEE 802.15.4/802.11 and Sub-GHz technologies. IEEE Internet Things J 5(2):784–793. https://doi.org/10.1109/JIOT.2017.2747900

Di Marco P, Park P, Fischione C, Johansson KH (2010) Analytical modelling of IEEE 802.15.4 for multi-hop networks with heterogeneous traffic and hidden terminals, GLOBECOM—IEEE Glob Telecommun Conf 1–6. Doi:https://doi.org/10.1109/GLOCOM.2010.5683811.

El-Fouly FH, Ramadan RA (2020) Real-time energy-efficient reliable traffic aware routing for industrial wireless sensor networks. IEEE Access 8:58130–58145. https://doi.org/10.1109/ACCESS.2020.2980682

Farag H, Gidlund M, Österberg P (2018) A delay-bounded mac protocol for mission- and time-critical applications in industrial wireless sensor networks. IEEE Sens J 18(6):2607–2616. https://doi.org/10.1109/JSEN.2018.2793946

Fraile LP, Tsampas S, Mylonas G, Amaxilatis D (2020) A comparative study of LoRa and IEEE 802.15.4-based IoT deployments inside school buildings. IEEE Access 8:160957–160981. https://doi.org/10.1109/ACCESS.2020.3020685

Gezer A, Okdem S (2020) Improving IEEE 802.15.4 channel access performance for IoT and WSN devices. Comput Electr Eng. https://doi.org/10.1016/j.compeleceng.2020.106745

Hadadian Nejad Yousefi H, Kavian YS, Mahmoudi A (2019a) A markov model for investigating the impact of IEEE 802.15.4 MAC layer parameters and number of clusters on the performance of wireless sensor networks. Wirel Netw 25(7):4415–4430. https://doi.org/10.1007/s11276-019-02105-4

Hadadian Nejad Yousefi M, Kavian YS, Mahmoudi A (2019b) RTMCH: real-time multichannel MAC for wireless video sensor networks. Multimed Tools Appl 78(6):7803–7818. https://doi.org/10.1007/s11042-018-6480-9

IEEE Standard Association (2015) IEEE Get Program, (n.d.). http://standards.ieee.org/getieee802/download/802.15.4-2015.pdf.

Khanafer M, Guennoun M, Mouftah HT (2014) A survey of beacon-enabled IEEE 802154 MAC protocols in wireless sensor networks. IEEE Commun Surv Tutor 16(2):856–876. https://doi.org/10.1109/SURV.2013.112613.00094

Kim TO, Kim H, Lee J, Park JS, Choi BD (2006) Performance analysis of IEEE 802.15.4 with non-beacon-enabled CSMA/CA in non-saturated condition. In: Sha E, Han SK, Xu CZ, Kim MH, Yang LT, Xiao B (eds) Embedded and ubiquitous computing. EUC 2006. Lecture notes in computer science, vol 4096. Springer, Berlin. https://doi.org/10.1007/11802167_89

Kim TO, Park JS, Kim KJ, Choi BD (2009) Performance analysis of IEEE 802154 non-beacon mode with both uplink and downlink traffic in non-saturated condition. In: Granelli F, Skianis C, Chatzimisios P, Xiao Y, Redana S (eds) Mobile lightweight wireless systems. Mobilight 2009. Lecture notes of the institute for computer sciences, social informatics and telecommunications engineering, vol 13. Springer, Berlin, pp 357–371. https://doi.org/10.1007/978-3-642-03819-8_34

Kim TO, Baek S, Choi BD (2016) Performance analysis of IEEE 802.15.4 superframe structure with the inactive period. Perform Eval 106:50–69. https://doi.org/10.1016/j.peva.2016.10.002

Kobayashi K (2015) LAWIN: A Latency-AWare InterNet architecture for latency support on best-effort networks, IEEE 16th international conference on high performance switching and routing (HPSR), Budapest, 2015: 1–8. doi: https://doi.org/10.1109/HPSR.2015.7483104.

Koyuncu M, Yazici A, Civelek M, Cosar A, Sert M (2019) Visual and auditory data fusion for energy-efficient and improved object recognition in wireless multimedia sensor networks. IEEE Sens J 19(5):1839–1849. https://doi.org/10.1109/JSEN.2018.2885281

Li X, Li D, Wan J, Vasilakos AV, Lai C-F, Wang S (2017) A review of industrial wireless networks in the context of Industry 4.0. Wirel Netw 23(1):23–41. https://doi.org/10.1007/s11276-015-1133-7

Martalò M, Busanelli S, Ferrari G (2009) Markov Chain-based performance analysis of multihop IEEE 802.15.4 wireless networks. Perform Eval 66:722–741. https://doi.org/10.1016/j.peva.2009.08.011

Misic J, Misic VB, Shafi S (2004) Performance of IEEE 802154 beacon enabled PAN with uplink transmissions in non-saturation mode—access delay for finite buffers. In: First Int Conf Broadband Networks, IEEE Comput Soc, pp 416–425. doi:https://doi.org/10.1109/BROADNETS.2004.61

Misic J, Shafi S, Misic VB (2006) Performance of a beacon enabled IEEE 802154 cluster with downlink and uplink traffic. IEEE Trans Parallel Distrib Syst 17(4):361–376. https://doi.org/10.1109/TPDS.2006.54

Moulik S, Misra S, Chakraborty C (2019) Performance evaluation and delay-power trade-off analysis of ZigBee protocol. IEEE Trans Mob Comput. https://doi.org/10.1109/TMC.2018.2836456

Park P, Di Marco P, Fischione C, Johansson KH (2013) Modeling and optimization of the IEEE 802.15.4 protocol for reliable and timely communications. IEEE Trans Parallel Distrib Syst 24(3):550–564. https://doi.org/10.1109/TPDS.2012.159

Pollin S, Ergen M, Ergen S, Bougard B, Der Perre L et al (2006) Performance analysis of slotted carrier sense IEEE 802.15.4 medium access layer. IEEE Globecom USA. https://doi.org/10.1109/GLOCOM.2006.672

Pollin S, Ergen M, Ergen S, Bougard B, Der Perre L, Moerman I, Bahai A, Varaiya P, Catthoor F (2008) Performance analysis of slotted carrier sense IEEE 802.15.4 medium access layer. IEEE Trans Wirel Commun 7:3359–3371. https://doi.org/10.1109/TWC.2008.060057

Quang PTA, Kim D (2012) Enhancing real-time delivery of gradient routing for industrial wireless sensor networks. IEEE Trans Ind Inf 8(1):61–68. https://doi.org/10.1109/TII.2011.2174249

Rahimifar A, Seifi Kavian Y, Kaabi H et al (2020) Predicting the energy consumption in software defined wireless sensor networks: a probabilistic Markov model approach. J Ambient Intell Hum Comput. https://doi.org/10.1007/s12652-020-02599-3

Raptis TP, Passarella A, Conti M (2019) Data management in industry 4.0: state of the art and open challenges. IEEE Access 7:97052–97093. https://doi.org/10.1109/ACCESS.2019.2929296

Rasouli H, Kavian YS, Rashvand HF (2014) ADCA: Adaptive duty cycle algorithm for energy efficient IEEE 802.15.4 beacon-enabled wireless sensor networks. IEEE Sens J 14(11):3893–3902. https://doi.org/10.1109/JSEN.2014.2353574

Schmitt JB, Zdarsky FA, Thiele L (2007) A comprehensive worst-case calculus for wireless sensor networks with in-network processing. Proc Real-Time Syst Symp 2007:193–202. https://doi.org/10.1109/RTSS.2007.17

Schütze A, Helwig N, Schneider T (2018) Sensors 4.0–smart sensors and measurement technology enable Industry 4.0. J Sens Sens Syst 7(1):359–371. https://doi.org/10.5194/jsss-7-359-2018

Sharif H, Kavian YS (2015) Technological breakthroughs in modern wireless sensor applications. IGI Glob. https://doi.org/10.4018/978-1-4666-8251-1

Tavallaie O, Naji HR, Sabaei M et al (2017) RTEA: real-time and energy aware routing for industrial wireless sensor networks. Wirel Pers Commun 95:4601–4621. https://doi.org/10.1007/s11277-017-4109-3

Wang Y, Vuran MC, Goddard S (2012) Cross-layer analysis of the end-to-end delay distribution in wireless sensor networks. IEEE/ACM Trans Netw 20(1):305–318. https://doi.org/10.1109/TNET.2011.2159845

Xu J, Guo C (2019) Scheduling periodic real-time traffic in lossy wireless networks as restless multi-armed bandit. IEEE Wirel Commun Lett 8(4):1129–1132. https://doi.org/10.1109/LWC.2019.2908905

Yadav DK, Karthik G, Jayanthu S, Das SK (2019) Design of real-time slope monitoring system using time-domain reflectometry with wireless sensor network. IEEE Sens Lett. https://doi.org/10.1109/LSENS.2019.2892435

Zheng M, Chen S, Liang W, Song M (2019) NSAC: a novel clustering protocol in cognitive radio sensor networks for internet of things. IEEE Internet Things J 6(3):5864–5865. https://doi.org/10.1109/JIOT.2019.2898166

Zhu J, Tao Z, Lv C (2012) Performance evaluation for a beacon enabled IEEE 802.15.4 scheme with heterogeneous unsaturated conditions. AEU Int J Electron Commun 66:93–106. https://doi.org/10.1016/j.aeue.2011.05.008